ELSEVIER

Polymer 40 (1999) 3763–3772

polymer

Kinetics of styrene miniemulsion polymerization stabilized by nonionic surfactant/alkyl methacrylate

Chorng-Shyan Chern*, Yuh-Cherng Liou

Department of Chemical Engineering, National Taiwan University of Science and Technology, 43 Keelung Rd., Sec. 4, Taipei, Taiwan

Received 9 June 1998; accepted 13 August 1998

Abstract

The effects of various reaction parameters on the styrene miniemulsion polymerizations stabilized by nonylphenol polyethoxylate with an average of 40 ethylene oxide units per molecule (NP-40) and dodecyl methacrylate (DMA) at 80°C were investigated. These parameters include the concentrations of DMA ([DMA]), NP-40 ([NP-40]), sodium persulfate ([SPS]), and 2,2′-azobisisobutyronitrile ([AIBN]). A water-insoluble dye was also incorporated into the reaction system to gain a better understanding of the related particle nucleation mechanisms. The polymerization rate decreases with increasing [DMA], whereas it increases with increasing [NP-40], [SPS] and [AIBN]. Several competitive events (e.g. coalescence among the monomer droplets, nucleation in the monomer droplets and micelles, formation of particle nuclei in water, and particle growth) occur simultaneously in the course of polymerization. This is due to the fact that the steric stabilization effect provided by NP-40 is greatly reduced at 80°C and the CMC of the miniemulsion is far below the NP-40 concentrations used in this work. Mixed modes of particle nucleation are operative in this reaction system, but monomer droplet nucleation becomes more important by increasing [DMA] or decreasing [NP-40], [SPS] and [AIBN].

Keywords: Miniemulsion polymerization; Styrene; Kinetics

1. Introduction

In conventional styrene (STY) emulsion polymerization, particle nucleation taking place in the emulsified monomer droplets is generally considered insignificant as compared to micellar nucleation [1–4]. This is because these monomer droplets are incapable of competing effectively with the monomer-swollen micelles for oligomeric radicals generated in the aqueous phase due to the relatively small droplet–water interfacial area. Nevertheless, the average size of the homogenized monomer droplets may become small enough to allow these droplets to become the predominant particle nucleation loci. This process has been termed miniemulsion polymerization [5–8]. The monomer droplets can be stabilized by an anionic surfactant (e.g. sodium dodecyl sulfate (SDS)) or a nonionic surfactant (e.g. nonylphenol polyethoxylate with an average of 40 ethylene oxide units per molecule (NP-40)) to prevent these droplets from coalescing and a water-insoluble, low molecular weight cosurfactant (e.g. cetyl alcohol (CA) and hexadecane (HD)) to retard diffusion of monomer from small droplets to large ones (Ostwald ripening) [9].

In our previous work [10], an extremely hydrophobic alkyl methacrylate such as dodecyl methacrylate (DMA) or stearyl methacrylate (SMA) was used to replace the conventional cosurfactant in preparing relatively stable STY miniemulsions. Such a long chain alkyl methacrylate monomer can be chemically incorporated into the latex particles during the subsequent miniemulsion polymerization. During the reaction, the colloidal stability of the particles protected by SDS/DMA or SDS/SMA was quite satisfactory. Recently, the authors incorporated a tiny amount of a water-insoluble blue dye into the monomer droplets to study the particle nucleation mechanisms involved in the STY miniemulsion polymerizations stabilized by SDS/DMA or SDS/SMA [11]. Transport of these dye molecules from the monomer droplets, through the aqueous phase, and then into the growing particles was prohibited during polymerization due to their extremely low water solubility [12]. A mass balance was established to calculate the number of latex particles originating from the monomer droplets (N_d) and the number of primary particles generated in water. It should be noted that the accuracy of this method relies on producing a stable miniemulsion during polymerization. Mixed modes of particle nucleation (i.e. monomer droplet nucleation/homogeneous nucleation) were observed in the polymerization system. The surfactant

* Corresponding author. Tel.: + 886-2-27376649; Fax: + 886-2-27376644; e-mail: chern@ch.ntust.edu.tw

0032-3861/99/$ - see front matter
PII: S0032-3861(98)00599-0

species required to stabilize the particle nuclei formed in water may come from those dissolved in water or even those adsorbed on the monomer droplet surfaces.

In contrast to the electrostatic stabilization provided by the anionic surfactant SDS [13,14], the nonionic surfactant NP-40 imparts steric repulsion force between two interactive hairy particles [15,16]. The latex products stabilized by nonionic surfactants are quite insensitive to changes in the ionic strength of the aqueous solution. In addition, NP-40 can improve the chemical and freeze–thaw stability of the latex products. Thus, NP-40 has been widely used in the production of various emulsion polymers. In a previous report [17], stable STY miniemulsions with NP-40 in combination with various cosurfactants (CA, HD, DMA and SMA) were prepared and characterized. The rate of Ostwald ripening for these miniemulsions in decreasing order is: CA > DMA > HD ≅ SMA. This trend correlates well with the water solubility of these cosurfactants. That is, the more hydrophobic the cosurfactant, the more effective is the cosurfactant in retarding the diffusional degradation of monomer droplets. It was concluded that latex particles formed via both monomer droplet nucleation and homogeneous (or micellar) nucleation for the miniemulsions exhibiting strong Ostwald ripening and/or droplet coalescence during the very early stage of polymerization. On the other hand, monomer droplet nucleation became more important for the miniemulsions showing weak Ostwald ripening. The objective of this continuous project was to investigate the kinetics of STY miniemulsion polymerization stabilized by NP-40/DMA. Furthermore, a water-insoluble blue dye (0.1% based on total monomer weight throughout this work) was incorporated into the monomer droplets to gain a better understanding of the particle nucleation loci involved in this reaction system.

2. Experimental

The chemicals used in this work include styrene (STY) (Acros), nonylphenol polyethoxylate with an average of 40 ethylene oxide units per molecule (NP-40) (Union Carbide), dodecyl methacrylate (DMA) (Aldrich), stearyl methacrylate (SMA) (Mitsubishi Rayon), sodium persulfate (SPS) (Riedel-de Haen), 2,2′-azobisisobutyronitrile (AIBN) (Mitsubishi Rayon), sodium bicarbonate (Riedel-de Haen), water-insoluble blue dye (Blue 70, Shenq-Fong Fine Chemical Ltd, China, $M_W \cong 10^3$ g/mol, its molecular structure is shown in Refs [11,12]), toluene (Acros), nitrogen (Ching-Feng-Harng Co.), and deionized water (Barnsted, Nanopure Ultrapure Water System, specific conductance < 0.057 μS/cm). The reagent SMA was recrystallized in ethanol and STY was distilled under reduced pressure before use. All other chemicals were used as received.

The miniemulsion was prepared by dissolving NP-40 in water and DMA (or SMA) in STY, respectively. The oily and aqueous solutions were mixed with a mechanical agitator at 400 rpm for 10 min. The resultant emulsion was then homogenized by the Microfluidizer-110Y (Microfluidics Co.), operated at 5000 psi outlet pressure and 10 passes. Miniemulsion polymerization was carried out in a 250 ml reactor equipped with a four-bladed fan turbine agitator, a thermometer and a reflux condenser. Immediately after homogenization, the resultant miniemulsion was charged into the reactor and then purged with nitrogen for 10 min while the reactor temperature was raised to 80°C. A typical miniemulsion charge (designated as NP2) comprises 165 g water, 0.036 g sodium bicarbonate (2.66 mM based on total water), 1.634 g NP-40 (5 mM based on total water), 0.838 g DMA (20 mM based on total water), 0.04 g dye (0.24 mM based on total water), 0.209 g SPS (5.32 mM based on total water), and 40 g STY. The theoretical solid content of the latex product is 20.6%. The finished batch was filtered through 40-mesh (0.42 mm) and 200-mesh (0.074 mm) screens in series to collect the filterable solids. Scraps adhering to the agitator, thermometer and reactor wall were also collected. Total solid content and conversion of STY were determined gravimetrically.

The data of average monomer droplet size (or latex particle size) were obtained from the dynamic light scattering method (Otsuka Photal LPA-3000/3100). The sample was diluted with water to adjust the number of photons counted per second (cps) to 8000–12 000. The dilution water was saturated with NP-40 (critical micelle concentration, (CMC) = 0.29 mM at 25°C) and STY (1.92 mM) to avoid diffusion of NP-40 and STY from the monomer droplets (or monomer-swollen latex particles) into water. The CMC data for NP-40 at 25°C and the water solubility data for STY were taken from Refs [18,19], respectively. The reported monomer droplet size data represent an average of at least three measurements and the errors have been estimated to be 8% or less. From the average monomer droplet size immediately before the start of polymerization ($d_{m,i}$) and the average size of the resultant latex particles ($d_{p,f}$), the number of monomer droplets per liter of water formed immediately before the start of polymerization ($N_{m,i}$) and the number of latex particles per liter of water produced at the end of polymerization ($N_{p,f}$) were then calculated.

The following procedure developed in Refs [11,12] was used to determine the dye content in the resultant latex particles. A distinct peak at 678 nm was observed for the solution of 1.7×10^{-4} g dye and 0.2 g dried polystyrene in 20 ml toluene by the UV absorbance method (Shimadzu, UV-160A). No absorbance was detected at this wavelength for the solution of 0.2 g dried polystyrene in 20 ml toluene. The extinction coefficient obtained from the calibration curve of the UV absorbance at 678 nm versus the dye concentration data was determined to be 8.2765×10^4 ml/cm g. To determine the amount of dye ultimately incorporated into the latex particles, the latex product was allowed to stand at 25°C over 3 days before UV absorbance measurements. In this manner, a thin layer of blue precipitate (originating from the bulk dye suspended in

Table 1
Results obtained from the styrene miniemulsion polymerizations stabilized by nonionic surfactant/alkyl methacrylate

Exp ID	NP1	NP2	NP3	NP4	NP5	NP6	NP7	NP8	NP9	NP10	NP11	NP12
[NP-40] (mM)	5	5	5	1	10	5	5	5	5	5	5	5
[DMA] (mM)	5	20	40	20	20	20	20	20	20	20	20	
[SMA] (mM)												20
[SPS] (mM)	5.32	5.32	5.32	5.32	5.32	7.98	2.66	7.98				5.32
[AIBN] (mM)									5.59	11.17	16.76	
T (°C)	80	80	80	80	80	80	80	70	80	80	80	80
$d_{m,i}$ (nm)	257.8	207.9	169.5	276.5	188.6	188.8	184.7	157.0	159.8	159.8	150.0	135.6
$d_{p,f}$ (nm)	211.6	240.1	232.2	390.1	202.1	235.4	236.8	237.2	191.4	191.4	202.3	189.0
$N_{m,i} \times 10^{-16}$ (1/L)	3.00	5.72	10.55	2.43	7.66	7.63	8.15	13.28	12.59	11.60	15.22	20.61
$N_{p,f} \times 10^{-16}$ (1/L)	4.73	3.25	3.59	0.76	6.68	3.43	3.41	3.38	6.54	4.45	5.43	6.64
$N_{p,f}/N_{m,i}$	1.579	0.568	0.340	0.314	0.873	0.449	0.419	0.254	0.520	0.383	0.357	0.322
$R_p \times 10^2$ (mol/L min)	1.098	0.847	0.809	0.638	1.027	1.116	0.628	0.570	0.673	0.992	1.217	1.010
$R_p/N_{p,f} \times 10^{19}$ (mol/min)	3.321	2.609	2.254	8.372	1.536	3.256	1.839	1.690	1.029	2.231	2.240	1.522
P_{dye} (%)	39.14	46.81	47.75	48.03	40.71	43.76	59.14	37.20	66.35	56.60	49.81	49.09
Total scrap (%)	0.050	0.18	0.11	0.97	0.025	0.10	0.054	0.119	1.744	1.568	1.364	0.219

the latex product) can be found on the bottom of the sample. Approximately 2 g latex sample was pipetted from the middle portion of the sample and then dried in an oven. Subsequently, the dried polymer particles were dissolved in 20 ml toluene for determination of the dye content based on the above calibration curve.

3. Results and discussion

3.1. Effect of the DMA concentration

In this series of experiments, the concentrations of NP-40 ([NP-40]) and SPS ([SPS]) were kept constant at 5 and 5.32 mM based on total water, respectively. The polymerization temperature was kept constant at 80°C, which is widely used in the industrial production of latex products using the thermally decomposed persulfate initiator (half life $\approx$ 0.5 h). The concentration of DMA ([DMA]) was varied from 5 to 40 mM based on total water (see NP1, NP2 and NP3 in Table 1). The $d_{m,i}$ and $N_{m,i}$ data are summarized in Table 1. It is shown that $d_{m,i}$ decreases and, therefore, $N_{m,i}$ increases with increasing [DMA]. This is due to the fact that the Ostwald ripening rate is inversely proportional to the volume fraction of cosurfactant in the droplet according to the modified LSW theory [9]. Thus, under the same homogenization condition, the higher the DMA concentration, the smaller are the resultant monomer droplets.

Fig. 1a shows the monomer conversion (X) as a function of time (t) for the runs with various levels of DMA. The polymerization rate ($R_p = [M]_0 dX/dt$) data in Table 1 show that R_p decreases with increasing [DMA], in which $[M]_0$ is the initial monomer concentration based on total water (2.33 mM) and the value of dX/dt is the least-squares-best-fitted slope of the linear portion of the X versus t curve. However, as shown in Table 1, there is no apparent correlation between R_p and $N_{p,f}$, which is presumably caused by the very complicated reaction mechanisms involved in this system. Thus, $N_{p,f}$ does not necessarily represent the number of reaction loci during the constant polymerization rate region. In addition, the colloidal stability of the latex particles is satisfactory during the reaction, as reflected by the relatively low levels of coagulum collected at the end of polymerization (see the total scrap data in Table 1). The average particle size (d) versus t data for the runs with [DMA] = 5–40 mM are shown in Fig. 1b. It should be noted that monomer droplets may coexist with the nucleated particles in the reaction system and, therefore, the dynamic light scattering data (d) only represent the average particle size of the reaction mixture consisting of both latex particles and monomer droplets.

For the run with the lowest [DMA] (5 mM), d decreases rapidly to a minimum at X = 15–20% (see Fig. 1a and b), followed by a gradual increase to a plateau. This trend was also observed in Ref. [17] and it was attributed to homogeneous nucleation [20–22]. The surfactant required to stabilize the primary particles nucleated in the aqueous phase comes from those dissolved in water and those released from monomer droplet surfaces. Nevertheless, the micellar nucleation mechanism [1–4] cannot be ruled out because [NP-40] is one order of magnitude greater than its CMC (0.152 mM at 80°C) [18] and, therefore, micelles may be present in the reaction system. Recently, Lin et al. [23] used a 4-terminal cell and an impedance spectrometer to determine the CMC of a similar ST miniemulsion containing various levels of SDS and 20 mM DMA. They found that the CMC of the miniemulsion with a diameter of 270 nm was about five times as large as that of the SDS aqueous solution. The increased CMC was attributed to adsorption of SDS molecules on the huge monomer droplet–water interfacial area. The CMC of the miniemulsions with [NP-40] = 5 mM and [DMA] = 5–40 mM cannot be estimated since the saturated surface area covered by one NP-40 molecule on the STY droplet surface is not known. Judging from the molecular structures of SDS and NP-40, however, the saturated surface area of NP-40 is

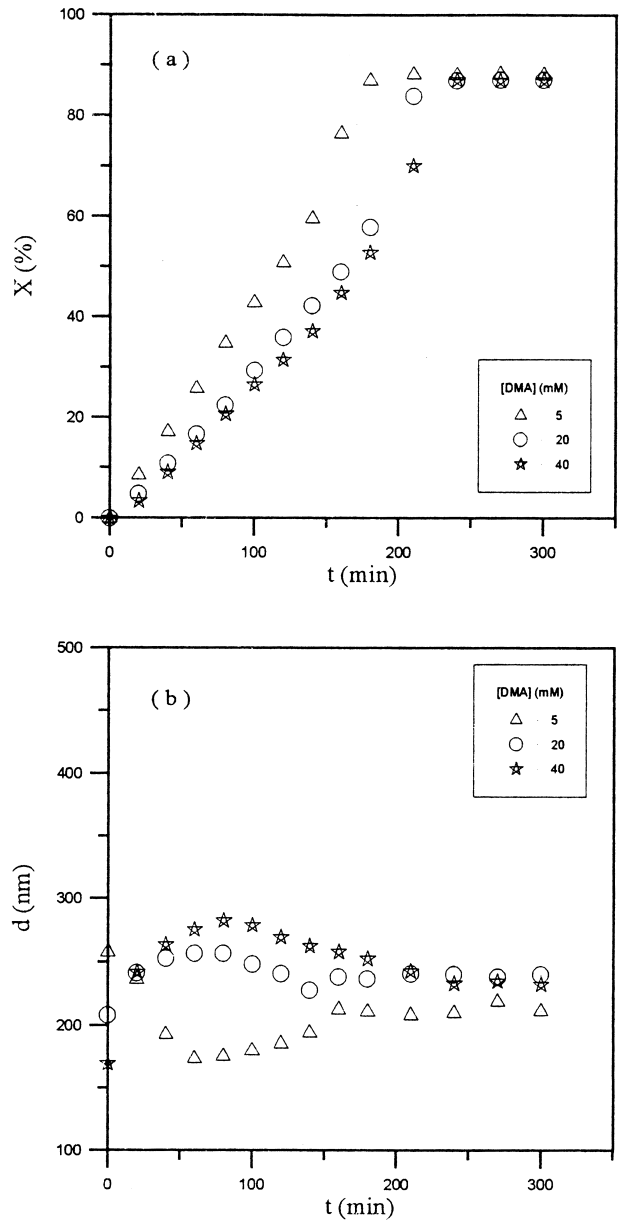

Fig. 1. (a) Monomer conversion and (b) average particle size as a function of the reaction time: [DMA] = (△) 5; (○) 20; (☆) 40 mM.

expected to be much larger than that of SDS. The reason for this prediction is that, under the saturated adsorption condition, the hydrophilic part of NP-40 (40 ethylene oxide units) may occupy a significant space near the droplet surface due to the excluded volume effect and the larger hydrophobe size of NP-40 (15 carbon atoms) in comparison with that of SDS (12 carbon atoms). This postulation is supported by the saturated particle surface area data reported for SDS (1.412×10^{21} nm^2/g) and NP-40 (0.238×10^{21}–0.480×10^{21} nm^2/g) adsorbed on the acrylic latex particles [24–27]. All these factors will cause a reduction in the amount of NP-40 adsorbed on the droplet surface as compared to SDS. At constant W_m and W_w, $N_{m,i} = W_m/(\pi/6\, d_{m,i}^3 \rho_m W_w) = C_1 1/d_{m,i}^3$ and $A_{m,i} = \pi d_{m,i}^2 N_{m,i} W_w = 6W_m/(d_{m,i}\rho_m) = C_2 1/d_{m,i}$. The parameters W_m, W_w, ρ_m and $A_{m,i}$ are the initial monomer weight, total water weight, monomer density and total monomer droplet surface area immediately before the start of polymerization, respectively, and C_1 and C_2 are proportional constants. Thus, the value obtained from the expression $0.152 \times 5 \times 270/169.5 = 1.211$ mM represents an upper limit for the CMC of the miniemulsion with [NP-40] = 5 mM and [DMA] = 40 mM. The numeric values of 0.152 (mM) and 169.5 (nm) are the CMC of the NP-40 solution and $d_{m,i}$ data, respectively. The ratio 270/169.5 represents the ratio of the monomer droplet surface area for the miniemulsion with [NP-40] = 0 mM to that for the miniemulsion prepared by Lin et al. [23]. The CMC of the miniemulsion with [NP-40] = 5 mM and [DMA] = 5 or 20 mM is expected to be lower than 1.211 mM because of the smaller droplet surface area available for adsorption of surfactant molecules. Under the circumstances, a significant population of micelles exists in the miniemulsion. Thus, the population of latex particles originating from micellar nucleation cannot be ignored during the particle nucleation process. How to quantitatively determine each fraction of the latex particles generated by various nucleation mechanisms then places a great challenge before polymer chemists.

After the minimal d is reached, the latex particles originating from homogeneous and micellar nucleation continue to grow in size by polymerizing the imbibed monomer provided by the unnucleated monomer droplets for the run with [DMA] = 5 mM. In addition, the rapidly growing particle surface area available for capturing oligomeric radicals and/or primary particles generated in water may severely depress particle nucleation in the aqueous phase. Another possible explanation is that the hydrogen bond between the polyethylene oxide part of NP-40 and water is greatly reduced at 80°C and, therefore, the hydrophilicity of NP-40 is lowered. This may impair the steric stabilization effect provided by NP-40 and cause coalescence among the interactive monomer droplets. As a consequence, d starts to increase gradually to a plateau as the experiment proceeds toward the end of polymerization (see Fig. 1b). The d versus t profile for the run with [DMA] = 5 mM suggests that formation of very small latex particles via micellar and homogeneous nucleation overrides the particle growth and droplet coalescence processes during the early stage of polymerization (X = 0–20%). On the other hand, the effects of micellar and homogeneous nucleation become insignificant as compared to the particle growth and droplet coalescence processes beyond 20% conversion.

In contrast to the run with [DMA] = 5% (NP1), d first increases to a maximum at X = 15–20% and then decreases to a plateau with the progress of polymerization for the run with [DMA] = 20 or 40 mM (NP2 or NP3) (see Fig. 1a and b). This opposite trend can be attributed to the following factors. First, the initial monomer droplet surface area in the decreasing order is NP3 > NP2 > NP1 because $d_{m,i}$ decreases with increasing [DMA]. The amount of NP-40

available for stabilizing the growing particles generated by micellar and homogeneous nucleation in the decreasing order is NP1 > NP2 > NP3. Thus, the effects of particle growth and droplet coalescence outweigh the effect of generation of tiny particles in water and inside the monomer-swollen micelles when $X < 15–20\%$. This will then result in an increase in d as the polymerization proceeds. Another consequence of such a droplet coalescence process is the shrinking droplet surface area overcrowded with NP-40. A fraction of the NP-40 molecules may thus desorb from the droplet surfaces. After the maximal d is reached, the level of the desorbed NP-40 may become high enough to protect the particle nuclei produced in water. As a result, d continues to decrease to a plateau beyond 15–20% conversion.

To verify the above postulation that the droplet coalescence process plays an important role in the NP-40 stabilized STY miniemulsion polymerization at 80°C, the more hydrophobic SMA was used to replace DMA. The reagent SMA was shown to be very effective in retarding the diffusional degradation of monomer droplets (Ostwald ripening) [10,17]. In these experiments, [NP-40], [SMA] (or [DMA]) and [SPS] were set at 5, 20 and 5.32 mM, respectively. Fig. 2a and b show the X versus t and d versus t curves, respectively, for the runs with different cosurfactants (DMA versus SMA) (also see NP2 and NP12 in Table 1). The polymerization rate for NP12 is faster than that for NP2 because the number of reaction loci (or $N_{p,f}$) for NP12 is about twice as large as that for NP2. A similar d versus t curve is also observed for the SMA containing system, which provides supporting evidence for the poor performance of NP-40 in stabilizing the droplets at 80°C. Another set of experiments was carried out to study the temperature effect (see NP6 and NP8 in Table 1). The values of [NP-40], [DMA] and [SPS] were kept constant at 5, 20 and 7.98 mM, respectively. The reaction temperature was set at 80 and 70°C for NP6 and NP8, respectively. Note that a higher level of SPS (7.98 instead of 5.32 mM) was used in order to obtain a reasonable R_p at 70°C. The data of X and d as a function of t for NP6 and NP8 are shown in Fig. 3a and b, respectively. As expected, R_p (NP6) is much faster than R_p (NP8), as shown in Fig. 3a and Table 1. It is very interesting to note that NP6 exhibits a similar d versus t profile to NP2 (see the circular data points in Fig. 1b and the triangular data points in Fig. 3b). On the other hand, for the run operated at 70°C, d increases steadily in the course of polymerization, primarily due to the continuous growth of latex particles. This result further confirms the sensitivity of the steric stabilization provided by NP-40 to changes in temperature. Consequently, coalescence of the droplets becomes more important when the temperature is increased.

The ratio $N_{p,f}/N_{m,i}$ decreases with increasing [DMA] (see NP1, NP2 and NP3 in Table 1). Furthermore, $N_{p,f}/N_{m,i}$ is greater than 1 for the run with the lowest [DMA], NP1. This indicates that, in addition to monomer droplet nucleation, a significant fraction of latex particles is generated by

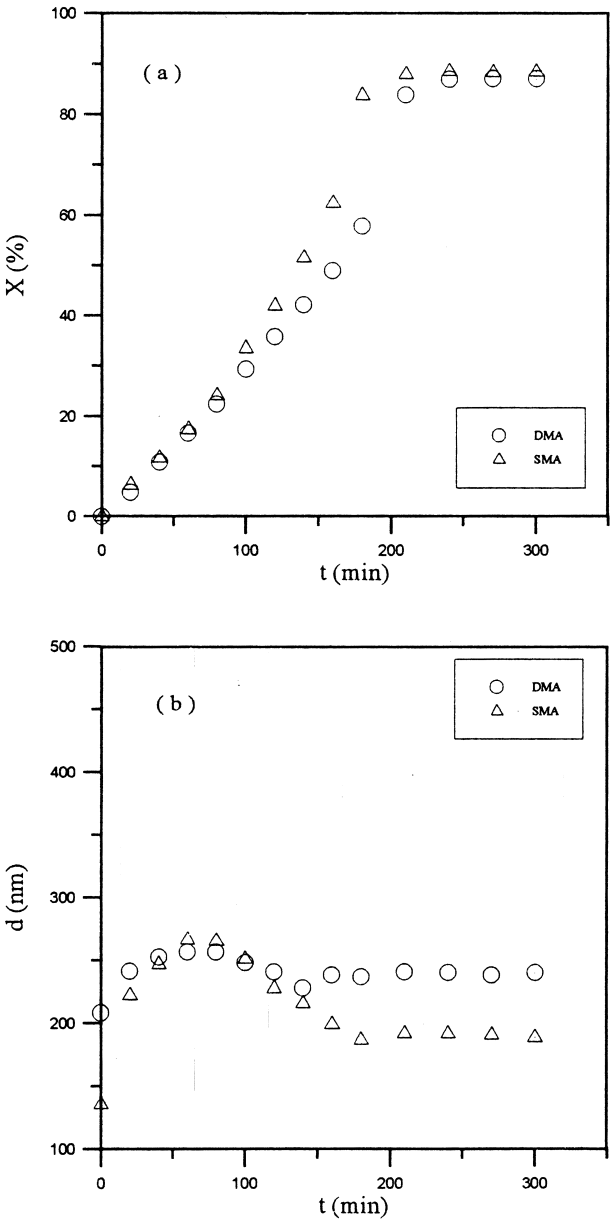

Fig. 2. (a) Monomer conversion and (b) average particle size as a function of the reaction time: (○) DMA; (△) SMA.

micellar and homogeneous nucleation. On the other hand, the values of $N_{p,f}/N_{m,i}$ for both NP2 and NP3 are less than 1. This may lead to the postulation that nucleation in the monomer droplets predominates the particle formation process. Recently, the authors used an extremely water-insoluble dye to study the particle nucleation mechanisms involved in the STY miniemulsion polymerizations stabilized by SDS/DMA or SDS/SMA [11]. The idea behind this technique is briefly described as follows. Immediately before the start of polymerization, most of the dye molecules are uniformly distributed among the monomer droplets and, perhaps, a small amount of dye is solubilized in the monomer-swollen micelles if micelles are present in the reaction system. The dye species can be incorporated

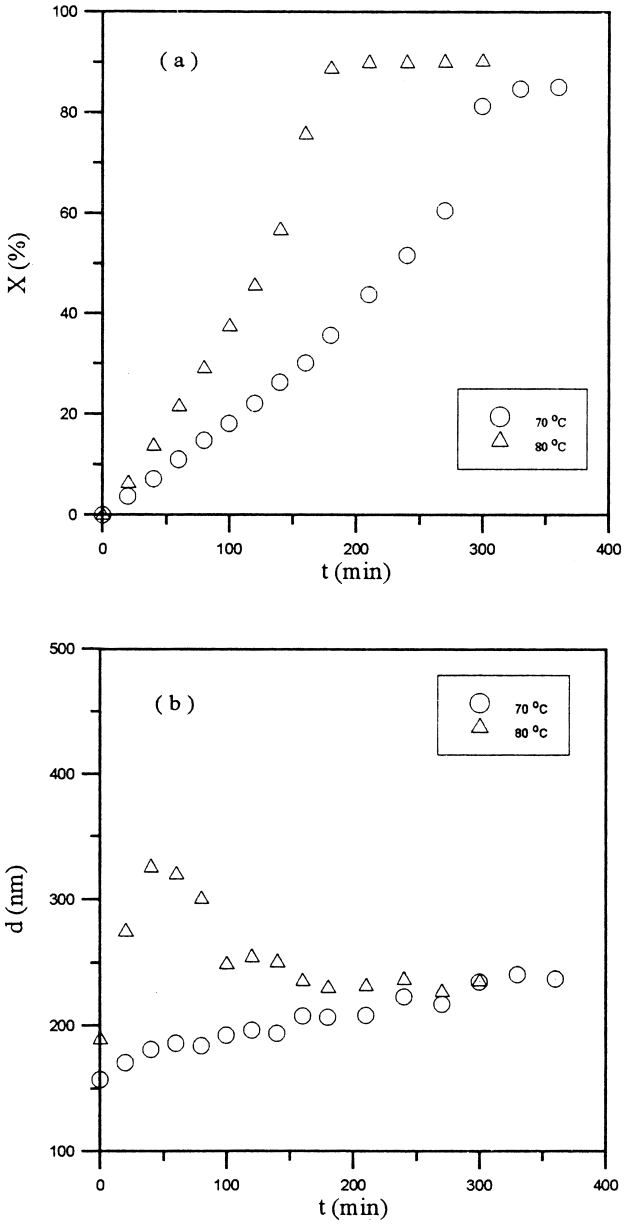

Fig. 3. (a) Monomer conversion and (b) average particle size as a function of the reaction time: (△) 80; (○) 70°C.

into the resultant latex particles only when oligomeric radicals enter the monomer droplets or micelles and successfully convert them into latex particles. The primary particles nucleated in the aqueous phase should not contain any dye species because transport of the extremely hydrophobic dye molecules from the monomer droplets, micelles or latex particles, across the aqueous phase, and then into the primary particles originating from homogeneous nucleation is prohibited. The monomer droplets or micelles, which has not participated in the particle nucleation process, only serve as a reservoir to supply the growing particles with monomer and surfactant and the dye molecules originally present in these degraded droplets and micelles will ultimately become suspended as a bulk material in the aqueous phase. Thus, determination of the weight percentage of dye incorporated into the resultant latex particles (P_{dye}) may provide valuable information on the related particle nucleation mechanisms. However, the accuracy of this method relies on producing a stable miniemulsion during the reaction. Thus, the mass balance established in Ref. [11] to determine the fraction of latex particles originating from each particle nucleation mechanism cannot be applied to the current polymerization system with significant droplet coalescence. Thus, P_{dye} only serves as a qualitative indicator for the relative importance of each particle formation process. Table 1 shows that P_{dye} increases with increasing [DMA]. This trend suggests that increasing [DMA] can greatly retard Ostwald ripening and, thereby, enhances the probability of capturing oligomeric radicals from the aqueous phase by these droplets exhibiting larger surface area. Therefore, the extent of monomer droplet nucleation increases as [DMA] is increased. The P_{dye} data also show that less than 48% of the initial droplets can be successfully converted into latex particles. For NP1, P_{dye} (39.14%) is far below $N_{p,f}/N_{m,i} \times 100\%$ (157.90%). On the other hand, P_{dye} (47.28 ± 0.47%) is quite close to $N_{p,f}/N_{m,i} \times 100\%$ (45.4 ± 11.4%) for NP2 or NP3. Although the results obtained from this work are not conclusive due to the droplet coalescence process, all these data seem to suggest that monomer droplet nucleation becomes more important when [DMA] increases from 5 to 40 mM. The reagent SMA is more effective in promoting nucleation in the monomer droplets in comparison with DMA (see the $N_{p,f}/N_{m,i}$ and P_{dye} data for NP2 and NP12 in Table 1).

3.2. Effect of the NP-40 concentration

In this series of experiments, [DMA], [SPS] and the polymerization temperature were kept constant at 20 mM, 5.32 mM and 80°C, respectively, and [NP-40] was varied from 1 to 10 mM (see NP2, NP4 and NP5 in Table 1). The value of $d_{m,i}$ decreases significantly with increasing [NP-40] because more NP-40 molecules are available for stabilizing the oil–water interfacial area generated during homogenization. The X versus t and d versus t data are shown in Fig. 4a and b, respectively. The polymerization rate increases with increasing [NP-40], as shown in Fig. 4a and Table 1. Again, this trend is closely related to $N_{p,f}$. That is, the larger the number of reaction loci available for consuming the imbibed monomer, the faster is the polymerization rate.

Fig. 4b shows that these polymerizations with various levels of NP-40 exhibit a similar d versus t profile. The value of d first increases to a maximum and then decreases to a plateau as the polymerization proceeds. During the early stage of polymerization, the degree of coalescence among the droplets decreases rapidly with increasing [NP-40]. This is because the higher the NP-40 concentration, the stronger the steric repulsion force between two colliding droplets [15,16]. This is also reflected by the total scrap data in Table 1. The amount of coagulum decreases rapidly

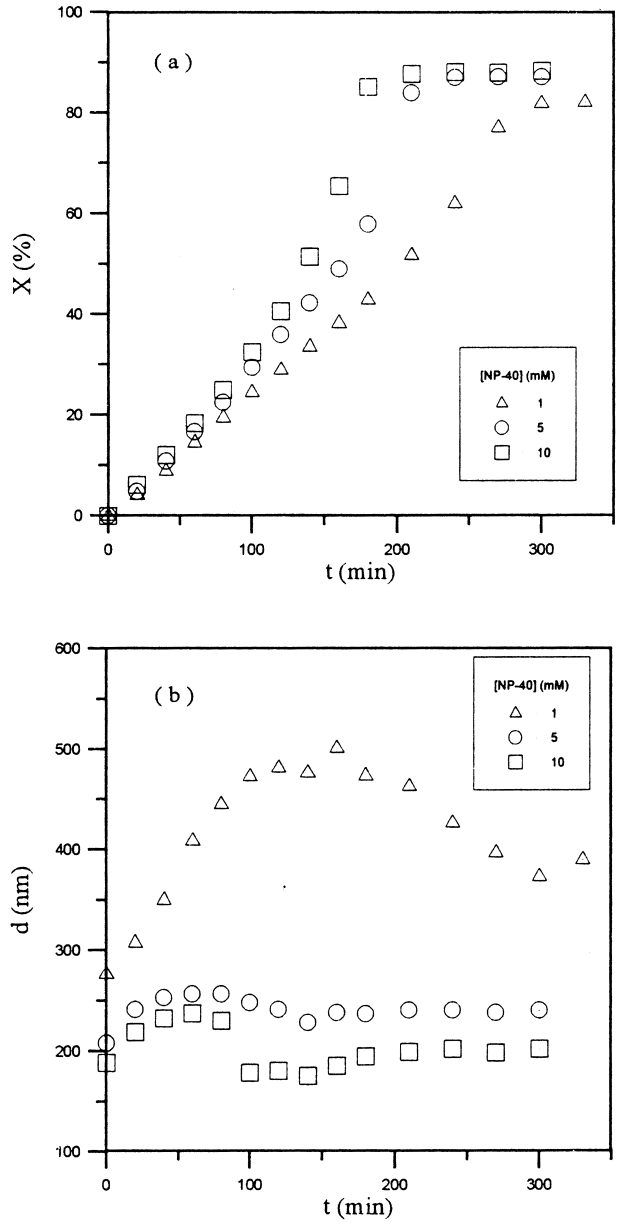

Fig. 4. (a) Monomer conversion and (b) average particle size as a function of the reaction time: [NP-40] = (△) 1; (○) 5; (□) 10 mM.

with increasing [NP-40]. The competitive reaction mechanisms proposed for NP2 and NP3 are responsible for the observed maximal d (see the section ''Effect of the DMA Concentration''). Table 1 shows that $N_{p,f}/N_{m,i}$ increases from 0.314 to 0.873, whereas P_{dye} decreases from 48.03 to 40.71% when [NP-40] increases from 1 to 10 mM. This result is most likely caused by the fact that the CMC of the miniemulsion with [NP-40] = 5 mM and [DMA] = 20 mM is in the order of 10^0 mM (see the section ''Effect of the DMA Concentration''). The concentration of micelles in the reaction mixture is then expected to increase significantly when [NP-40] increases from 1 to 10 mM. As a result, the fraction of latex particles originating from micellar and homogeneous nucleation increases as [NP-40] is increased.

3.3. Effect of the SPS concentration

In this series of experiments, [NP-40], [DMA] and the polymerization temperature were kept constant at 5 mM, 20 mM and 80°C, respectively, and [SPS] was varied from 2.66 to 7.98 mM (see NP2, NP6 and NP7 in Table 1). The value of $d_{m,i}$ (193.8 ± 14.1 nm) is insensitive to changes in [SPS] because the ionic strength of the aqueous medium does not show an appreciable influence on the performance of NP-40 (see Table 1). The data of X and d as a function of t are illustrated in Fig. 5a and b, respectively. As expected, R_p increases rapidly with increasing [SPS] (see Fig. 5a and Table 1). Interestingly enough, no apparent correlation exists between R_p and $N_{p,f}$ in this series of polymerizations (see Table 1). The increased R_p is attributed to the increased average number of free radicals per particle (n) with increasing [SPS]. This argument is further supported by the $R_p/N_{p,f}$ ($= k_p[M]_p/N_a$) data shown in Table 1, in which k_p is the propagation rate constant (2.052×10^4 l/mol min) [28], $[M]_p$ is the monomer concentration in the latex particles, and N_a is Avogadro's number. The ratio $R_p/N_{p,f}$ increases from 1.839×10^{-19} to 3.256×10^{-19} mol/min when [SPS] increases from 2.66 to 7.98 mM. Thus, $[M]_p n$ increases from 5.398 to 9.557 mol/l as [SPS] is increased from 2.66 to 7.98 mM. The value of $[M]_p$ is very difficult to predict because $[M]_p$ will decrease with increasing X and latex particles are generated via various nucleation mechanisms. Nevertheless, it seems reasonable to postulate that n increases with increasing [SPS] based on the $R_p/N_{p,f}$ data.

Fig. 5b shows that d first increases to a maximum and then decreases to a constant level ($d_{p,f} = 237.4 \pm 2.7$ nm, as shown in Table 1). Moreover, the peak observed in the d versus t curve becomes more prominent when [SPS] increases from 2.66 to 7.98 mM. This trend is probably due to the fact that more oligomeric radicals are produced in water at a higher level of SPS. This will then increase the probability of generating latex particles via micellar or homogeneous nucleation. These newly born particles compete effectively with the monomer droplets for NP-40 molecules and, thereby, promote the droplet coalescence process. As a result, the maximal d is the largest for the run with [SPS] = 7.98 mM. Table 1 shows that $N_{p,f}/N_{m,i}$ does not correlate well with [SPS], but P_{dye} decreases significantly with increasing [SPS]. The reduced P_{dye} with [SPS] is attributed to the increased number of latex particles formed via micellar or homogeneous nucleation.

3.4. Effect of the AIBN concentration

In the last series of experiments, [NP-40], [DMA] and the polymerization temperature were also kept constant at 5 mM, 20 mM and 80°C, respectively, but the water-soluble SPS was replaced by an oil-soluble initiator AIBN. The AIBN concentration ([AIBN]) was varied from 5.59 to

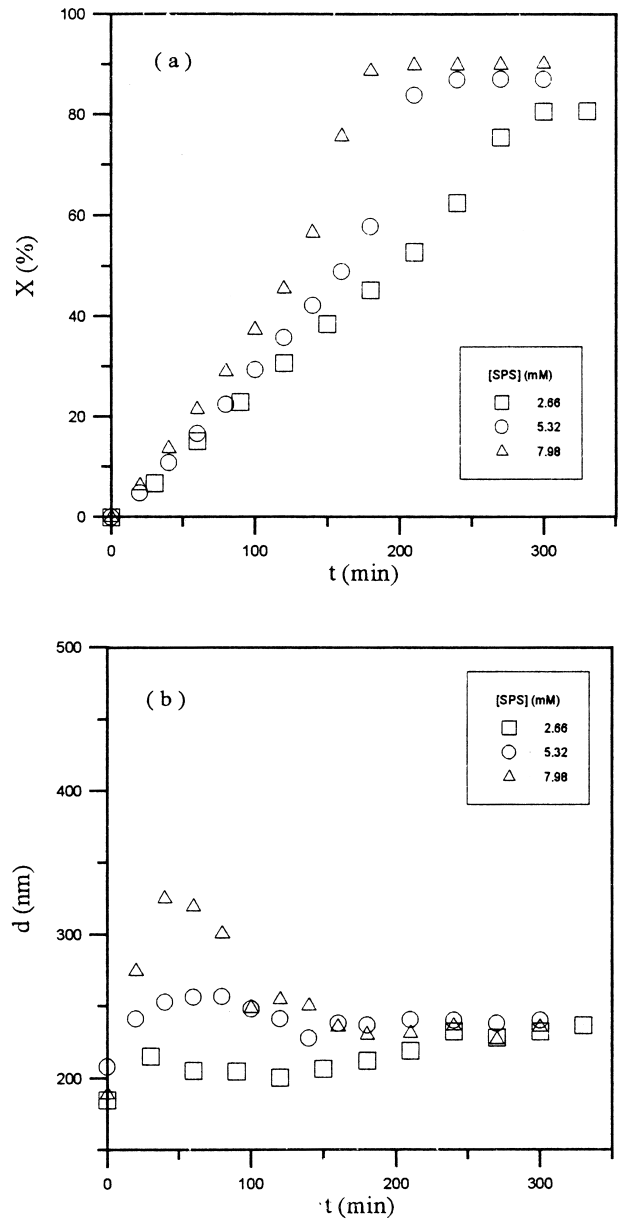

Fig. 5. (a) Monomer conversion and (b) average particle size as a function of the reaction time: [SPS] = (□) 2.66; (○) 5.32; (△) 7.98 mM.

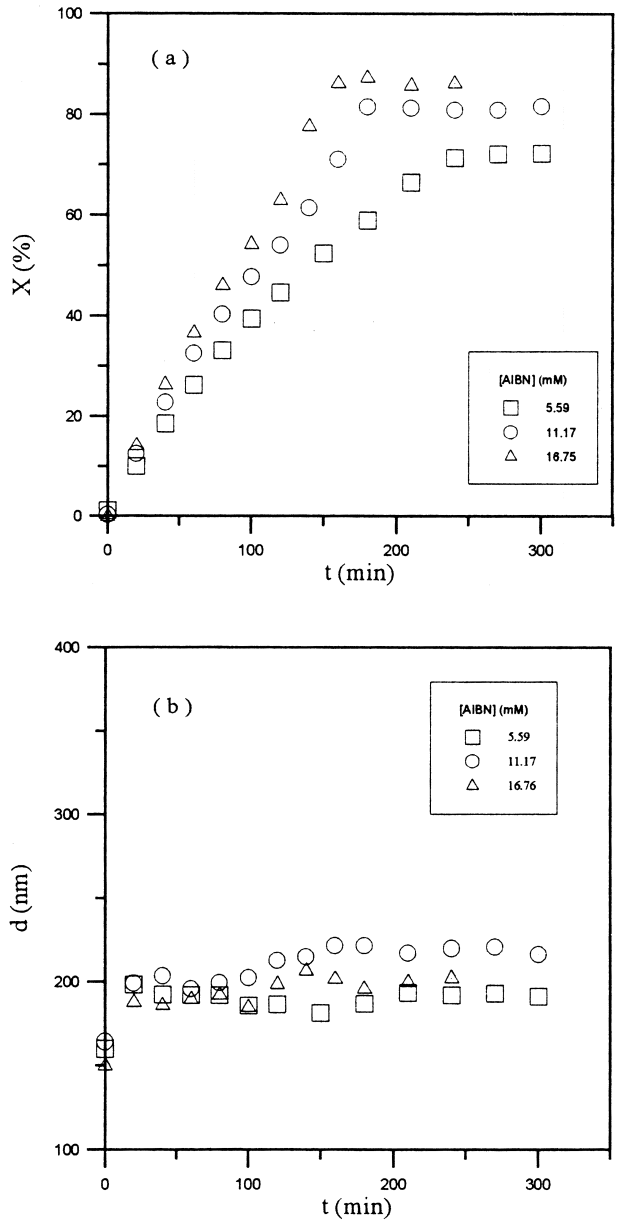

Fig. 6. (a) Monomer conversion and (b) average particle size as a function of the reaction time: [AIBN] = (□) 5.59; (○) 11.17; (△) 16.76 mM.

16.76 mM (see NP9, NP10 and NP11 in Table 1). Again, it is shown in Table 1 that $d_{m,i}$ (158.0 ± 8.0 nm) is independent of [AIBN]. The profiles of X versus t and d versus t are shown in Fig. 6a and b, respectively. Fig. 6a and Table 1 show that R_p increases with increasing [AIBN]. This is because the higher the AIBN concentration, the larger the value of n, as supported by the $R_p/N_{p,f}$ data in Table 1. It is interest to note that the total scrap (1.559 ± 0.195%) for the runs using AIBN as the initiator is quite high as compared to the runs with various levels of SPS (see Table 1). The reason for the reduced colloidal stability of the AIBN initiated STY miniemulsion polymerizations is not clear at this time.

Fig. 6b shows that for the AIBN containing reaction system d increases rapidly to a plateau as the polymerization proceeds, which is different from the SPS containing system. Similar to the polymerizations initiated by SPS, $d_{p,f}$ (203.5 ± 13.2 nm) is not sensitive to changes in [AIBN] (see Table 1). Both $N_{p,f}/N_{m,i}$ and P_{dye} decrease with increasing [AIBN] (see Table 1). These data imply that the fraction of AIBN dissolved in water may play an important role in the particle formation process. Although a pair of AIBN radicals tend to terminate with each other immediately after the initiator decomposition reaction taking place in the extremely small micelles (10^1 nm) (termed the cage effect), these micelles may be converted into latex particles by capturing oligomeric radicals in the aqueous phase. These oligomeric radicals may originate from the AIBN molecules dissolved in water or the

desorbed monomeric radicals via the chain transfer reaction occurring in the growing particles. This postulation is consistent with the reaction mechanism proposed for the conventional emulsion polymerizations with AIBN [29–32]. It is also interesting to note that the maximal P_{dye} obtained from this series of experiments is only 66.35%. This result indicates that not all the monomer droplets initially present in the reaction mixture can be successfully transformed into latex particles. However, the AIBN species are uniformly distributed in the monomer droplets just before the start of polymerization. Thus, the cage effect must have occurred in the smaller monomer droplets and these unnucleated droplets only serve as a reservoir of monomer and surfactant for the growing particles.

4. Conclusions

For the STY miniemulsion polymerization stabilized by NP-40 and DMA at 80°C, $d_{m,i}$ decreases with increasing [DMA]. The polymerization rate decreases with increasing [DMA]. The value of d first decreases rapidly to a minimum and then increases to a plateau as the polymerization proceeds for the run with the lowest level of DMA (5 mM). On the other hand, an opposite trend is observed for the run with a higher [DMA] (20 or 40 mM). The d versus t profile is governed by several competitive events such as the coalescence of the monomer droplets, nucleation in the monomer droplets and monomer-swollen micelles, formation of particle nuclei in the aqueous phase, and particle growth. This is caused by the fact that the steric stabilization effect provided by NP-40 is greatly reduced at 80°C and the CMC of the miniemulsion is far below the NP-40 concentrations used. The data of $N_{p,f}/N_{m,i}$ and P_{dye} show that the degree of monomer droplet nucleation increases with increasing [DMA].

The value of $d_{m,i}$ decreases and R_p increases with increasing [NP-40]. A similar d versus t curve is observed for the polymerizations with various levels of NP-40. The value of d first increases to a maximum and then decreases to a plateau as the polymerization proceeds. During the early stage of polymerization, the degree of coalescence among the monomer droplets decreases rapidly with increasing [NP-40]. The ratio $N_{p,f}/N_{m,i}$ increases and P_{dye} decreases when [NP-40] increases from 1 to 10 mM. This result is caused by the increased number of latex particles originating from micellar or homogeneous nucleation as [NP-40] is increased.

The value of $d_{m,i}$ is insensitive to changes in [SPS]. R_p increases rapidly with increasing [SPS]. This is due to the increased n with [SPS]. This trend is further supported by the $R_p/N_{p,f}$ data. For the polymerizations with various levels of SPS, d first increases to a maximum and then decreases to a constant level. Furthermore, the peak observed in the d versus t curve becomes more prominent as [SPS] is increased. The value of P_{dye} decreases significantly with increasing [SPS], which is attributed to the increased number of latex particles formed via micellar or homogeneous nucleation. In addition to SPS, the oil-soluble AIBN was also included in this work. Similarly, $d_{m,i}$ is independent of [AIBN]. R_p increases with increasing [AIBN]. This is because the higher the AIBN concentration, the larger the value of n. For the AIBN containing reaction system, d increases rapidly to a plateau as the polymerization proceeds, which is quite different from the SPS containing system. Both $N_{p,f}/N_{m,i}$ and P_{dye} decrease with increasing [AIBN]. These data imply that the fraction of AIBN dissolved in water may play an important role in the particle formation process. The maximal P_{dye} obtained from the AIBN initiated polymerizations is only 66.35%. This result indicates that not all the monomer droplets initially present in the reaction mixture can be successfully transformed into latex particles.

Acknowledgements

Financial support from the National Science Council, Taiwan is gratefully acknowledged.

References

[1] Harkins WD. J Am Chem Soc 1947;69:1428.
[2] Smith WV, Ewart RW. J Chem Phys 1948;16:592.
[3] Smith WV. J Am Chem Soc 1948;70:3695.
[4] Smith WV. J Am Chem Soc 1949;71:4077.
[5] Ugelstad J, El-Aasser MS, Vanderhoff JW. Polym Lett 1973;11:503.
[6] Ugelstad J, Hansen FK, Lange S. Die Makromol Chem 1974;175:507.
[7] Durbin DP, El-Aasser MS, Sudol ED, Vanderhoff JW. J Appl Polym Sci 1979;24:703.
[8] Chamberlain BJ, Napper DH, Gilbert RG. J Chem Soc Faraday Trans 1982;78:591.
[9] Kabalnov AS, Shchukin ED. Adv Colloid Interface Sci 1992;38:69.
[10] Chern CS, Chen T. J Colloid Polym Sci 1997;275:546.
[11] Chern CS, Liou YC, Chen TJ. Macromol Chem Phys 1998;199:1315.
[12] Chern CS, Chen TJ, Liou YC. Polymer 1998;39:3767.
[13] Deryagnin BV, Landau LD. Acta Physicochim USSR 1941;14:633.
[14] Verwey EJW, Overbeek JThG. Theory of the stability of lyophobic colloids. New York: Elsevier, 1943.
[15] Sato T, Ruch R. Stabilization of colloidal dispersions by polymer adsorption. New York: Marcel Dekker, 1980.
[16] Napper DH. Polymeric stabilization of colloidal dispersions. London: Academic Press, 1983.
[17] Chern CS, Chen T. J Colloid Polym Sci 1997;275:1060.
[18] Chen LJ, Lin SY, Chern CS, Wu SC. Colloids Surfaces A 1997;122:161.
[19] Sutterlin N. In: Fitch RM, editor. Polymer colloids II. New York: Plenum Press, 1980:583.
[20] Priest WJ. J Phys Chem 1952;56:1977.
[21] Fitch RM, Tsai CH. In: Fitch RM, editor. Polymer colloids. New York: Plenum Press, 1971:73.
[22] Fitch RM. Br Polym J 1973;5:467.
[23] Chang HC, Lin YY, Chern CS, Lin SY. Langmuir (in press).
[24] Sutterlin N. In: Fitch RM, editor. Polymer colloids II. New York: Plenum Press, 1971:583.
[25] Kronberg B, Stenius P. J Colloid Interface Sci 1984;102:410.
[26] Orr RJ, Breitman L. Can J Chem 1960;38:668.
[27] Chern CS, Hsu H. J Appl Polym Sci 1995;55:571.

[28] Matheson MS, Auer EE, Bevilacqua EB, Hart EJ. J Am Chem Soc 1949;71:497.
[29] Nomura M, Fujita K. Makromol Chem, Rapid Commun 1989;10:581.
[30] Nomura M, Yamada A, Fujita S, Sugimoto A, Ikoma J, Fujita K. J Polym Sci, Polym Chem Ed 1991;29:987.
[31] Nomura M, Ikoma J, Fujita K. J Polym Sci, Polym Chem Ed 1993;31:2103.
[32] Nomura M, Ikoma J, Fujita K. ACS Symp Ser 1992;492:55.